



Published in final edited form as:

*Mucosal Immunol.* 2010 January ; 3(1): 29–39. doi:10.1038/mi.2009.120.

## Novel signaling interactions between proteinase-activated receptor 2 and Toll-like receptors *in vitro* and *in vivo*

QM Nhu<sup>1,2</sup>, K Shirey<sup>1</sup>, JR Teijaro<sup>1</sup>, DL Farber<sup>1,3</sup>, S Netzel-Arnett<sup>4,5</sup>, TM Antalis<sup>2,4,5</sup>, A Fasano<sup>2</sup>, and SN Vogel<sup>1,2</sup>

<sup>1</sup>Department of Microbiology and Immunology, University of Maryland, Baltimore (UMB), School of Medicine, Baltimore, Maryland, USA.

<sup>2</sup>Mucosal Biology Research Center, University of Maryland, Baltimore (UMB), School of Medicine, Baltimore, Maryland, USA.

<sup>3</sup>Department of Surgery, University of Maryland, Baltimore (UMB), School of Medicine, Baltimore, Maryland, USA.

<sup>4</sup>Department of Physiology, University of Maryland, Baltimore (UMB), School of Medicine, Baltimore, Maryland, USA.

<sup>5</sup>Center for Vascular and Inflammatory Diseases, University of Maryland, Baltimore (UMB), School of Medicine, Baltimore, Maryland, USA.

### Abstract

Toll-like receptors (TLRs) and proteinase-activated receptors (PARs) function as innate immune biosensors in mucosal epithelial cells (ECs). We previously reported the functional and physical interactions between TLR4 and PAR<sub>2</sub>. We have extended these findings herein by showing the cooperation between PAR<sub>2</sub> and TLR2, TLR3, or TLR4 for activation of nuclear factor-κB-dependent signaling in mucosal EC lines. In contrast, activation of PAR<sub>2</sub> negatively regulated TLR3-dependent antiviral pathway, blunting the expression of TLR3/interferon regulatory factor-3 (IRF-3)-driven genes, as well as activation of IRF-3 and STAT1. Consistent with these *in vitro* observations, PAR<sub>2</sub><sup>-/-</sup> and TLR4<sup>-/-</sup> mice, which were refractory to footpad edema induced by PAR<sub>2</sub> agonist peptide, were protected from mouse-adapted H1N1 influenza A virus-induced lethality when compared to wild-type (WT) mice. These data support and extend our recently described, novel model of PAR<sub>2</sub>-TLR4 “receptor cooperativity” and highlight the complexity of signaling integration between heterologous innate immune biosensors.

### Keywords

proteinase-activated receptor 2; Toll-like receptor; IRF-3; interferon; H1N1 influenza A virus

### INTRODUCTION

Pathogen recognition is a critical function of innate immunity. Distinct germline-encoded pattern-recognition receptors (PRRs) expressed on innate immune cells detect microbial

---

**Correspondence:** Stefanie N. Vogel, Ph.D., Department of Microbiology and Immunology, University of Maryland, Baltimore, 685 W. Baltimore Street, Suite 380, Baltimore, MD 21201, USA, Tel: 410-706-4838; Fax: 410-706-8607, svogel@som.umaryland.edu.

### DISCLOSURE

The authors declared no conflict of interest.

structures and virulence factors, including microbial proteinases (reviewed in Gribar *et al.*<sup>1</sup> and Vroling *et al.*<sup>2</sup>). Toll-like receptors (TLRs) and proteinase-activated receptors (PARs) represent two structurally distinct classes of transmembrane receptors that have key roles in the innate immune response to pathogens. For example, influenza A virus infection activates multiple PRRs, including TLR3,<sup>3, 4</sup> but also generates extracellular proteinases<sup>5, 6</sup> that could activate PARs.

“Classical” PRRs sense pathogen-associated molecular patterns (PAMPs), structural molecular motifs that are evolutionarily conserved and shared among members of a given microbial class (reviewed in Janeway and Medzhitov,<sup>7</sup> Akira and Takeda,<sup>8</sup> and Akira *et al.*<sup>9</sup>). In mouse and man, the TLRs represent a family of >10 single-transmembrane classical PRRs that detect chemically conserved microbial components, for example, lipopolysaccharide (LPS), lipopeptides, and RNA. Ligand engagement of TLR N-terminal ectodomains induces receptor dimerization that brings the intracytoplasmic “Toll/interleukin-1 (IL-1) receptor resistance” (TIR) domains into close proximity. This interaction facilitates subsequent recruitment of TIR-domain-containing adapter proteins, kinases, and other signaling molecules to the “signaling platform” generated by the interacting TIR domains of the TLR dimer.

The innate immune system also senses proteolytic enzymes generated during infection through a family of “nonclassical” PRRs, for example, PARs. The PARs are a family of four 7-transmembrane, G protein-coupled receptors (7-TM GPCRs) that detect serine proteinases derived from pathogens and the host (reviewed in Steinhoff *et al.*<sup>10</sup> and Ramachandran and Hollenberg<sup>11</sup>). PAR<sub>1</sub>, PAR<sub>3</sub>, and PAR<sub>4</sub> are activated by thrombin; PAR<sub>2</sub> mediates the cellular effects of trypsin and trypsin-like enzymes, including several microbial proteinases. PAR-activating enzymes cleave each PAR irreversibly at a specific site in the extracellular N-terminus to expose a tethered neo-ligand that binds to the second extracellular loop (ECL2) of each GPCR to trigger receptor activation. In this sense, the PARs function as a novel class of nonclassical PRRs that might serve as additional pathogen/tissue damage biosensors. Synthetic PAR agonist peptides (AP), corresponding to the hexapeptide sequences of the tethered neo-ligands of PAR<sub>1</sub>, PAR<sub>2</sub>, and PAR<sub>4</sub>, activate the native, uncleaved PARs nonenzymatically by binding directly to the corresponding PAR ECL2 to mediate signaling.

Proteinase-activated receptors and TLRs are distributed ubiquitously, yet strategically, in the body. Of the four PARs, PAR<sub>2</sub> has been most extensively studied with respect to the inflammatory response to microbial exposure. PAR<sub>2</sub> is expressed highly in the respiratory and gastrointestinal (GI) tracts on epithelial cells (ECs), endothelial cells, macrophages, and dendritic cells (DCs) (reviewed in Steinhoff *et al.*<sup>10</sup> and Ramachandran and Hollenberg<sup>11</sup>). Exposure of human ECs to proteinases purified from certain pathogens activates PAR<sub>2</sub> to induce antimicrobial and inflammatory responses.<sup>12–15</sup> In mice, PAR<sub>2</sub> deficiency reduces clearance of bacterial, parasitic, and fungal infections.<sup>16–18</sup> Similar to PARs, TLRs are also expressed on ECs, endothelial cells, macrophages, and DCs in the airway and GI tract. In general, TLR2 and TLR4 recognize Gram-positive and Gram-negative bacteria, respectively; TLR3 detects double-stranded RNA (dsRNA) from viruses (reviewed in Akira and Takeda<sup>8</sup>). Experimentally, TLR2 is activated by synthetic di- or triacylated lipopeptides that mimic bacterial cell wall constituents. TLR3 is stimulated by the synthetic dsRNA analog, polyinosine-polycytidylic acid (poly I:C). TLR4 is triggered by Gram-negative bacterial LPS. Signals originating from independently engaged, heterologous receptors may converge synergistically or antagonistically to modify cellular responses to different exogenous stimuli (reviewed in Trinchieri and Sher<sup>19</sup> and O’Neill<sup>20</sup>). PAR<sub>2</sub> activation delivers intracellular signals that intersect with TLR/IL-1R signaling pathways.<sup>21–24</sup> We reported previously that PAR<sub>2</sub> AP augmented LPS-induced IL-8 secretion synergistically in SW620 human colonic ECs.<sup>23</sup> Our studies in HEK293T cells transfected with PAR<sub>2</sub> and/or TLR4 revealed a novel

mechanism of “receptor cooperativity” in which PAR<sub>2</sub> AP-induced NF-κB activation was synergistically enhanced by TLR4 coexpression.<sup>23</sup> These findings were strengthened by the observation that PAR<sub>2</sub> AP-induced NF-κB-dependent IL-1β mRNA expression in TLR4<sup>-/-</sup> macrophages was diminished.<sup>23</sup> Moreover, an AP-dependent, physical interaction between PAR<sub>2</sub> and TLR4 was shown in HEK293T cells by co-immunoprecipitation.<sup>23</sup>

Given that TLRs and PARs are concurrently present on mucosal ECs (reviewed in Vroling *et al.*), we hypothesized that intracellular signaling pathways utilized by TLRs and PAR<sub>2</sub> would converge either cooperatively or non-cooperatively when co-engaged. As the mucosal epithelium is the frontline innate immune barrier of the respiratory and GI tracts, we analyzed lung (A549) and colonic (SW620) ECs for responsiveness to stimulation of PAR<sub>2</sub> and/or TLRs. Specifically, cellular responses to agonists of TLR2, TLR3, or TLR4 were examined to determine the potential effects of PAR<sub>2</sub> activation on the inflammatory responses associated with bacterial and viral infections in mucosal ECs. Cooperation between PAR<sub>2</sub> and TLR2, TLR3, or TLR4 for nuclear factor-κB (NF-κB)-dependent IL-8 mRNA induction was observed. However, our data also revealed a novel role for PAR<sub>2</sub> in the negative regulation of TLR3 antiviral pathway, leading to reduced expression of TLR3-, interferon (IFN) regulatory factor-3 (IRF-3)-driven genes, and diminished activation of IRF-3 and signal transducer and activator of transcription 1 (STAT1). *In vivo*, both PAR<sub>2</sub><sup>-/-</sup> and TLR4<sup>-/-</sup> mice were highly refractory to footpad edema induced by PAR<sub>2</sub> AP, and less susceptible to lethality following intranasal infection with a mouse-adapted H1N1 influenza A virus than wild-type (WT) C57BL/6J mice. Collectively, this study highlights the complexity of signaling integration between heterologous innate immune biosensors that result in modulation of host inflammatory responses.

## RESULTS

We reported recently that PAR<sub>2</sub> AP synergized with the TLR4 agonist, LPS, to enhance IL-8 secretion in SW620 human colonic ECs.<sup>23</sup> As PAR<sub>2</sub> is expressed highly and strategically on ECs of the respiratory and GI tracts, we postulated that PAR<sub>2</sub> might function as a novel, nonclassical PRR. We also hypothesized that cross talk between the two heterologous PRR classes, that is, PAR<sub>2</sub> and TLR2, 3, and 4, would modulate the inflammatory response.

### PAR<sub>2</sub> AP responsiveness in human mucosal EC lines

Human lung (A549) and colonic (SW620) ECs were examined for responsiveness to PAR<sub>2</sub> AP. Both responded rapidly to PAR<sub>2</sub> AP with IL-8 mRNA induction that peaked rapidly at 0.5–1 h after stimulation (Figure 1a); SW620 ECs responded similarly, but somewhat less robustly than A549 ECs. PAR<sub>2</sub> AP-treated A549 ECs also expressed a broader array of proinflammatory mediator genes examined, for example, MIP-3α, tumor necrosis factor-α (TNF-α), IL-6, IL-8, MIP-2α, MCP-1, and COX-2 (Figure 1b) than SW620 ECs (data not shown). A549 and SW620 ECs responded to PAR<sub>2</sub> AP with peak AP activities at ~100 vs. ~300 μM, respectively (Figure 1c). A control, reverse peptide (RP) was inactive in both cell lines.

### Cooperative PAR<sub>2</sub>-TLR signaling integration in human mucosal EC lines

A549 and SW620 ECs were next examined for responsiveness to TLR2, TLR3, or TLR4 agonists, that is, Pam2CSK4 (or P2C), poly I:C, or LPS, respectively, in the absence or presence of PAR<sub>2</sub> AP. In both EC lines, PAR<sub>2</sub> AP enhanced IL-8 mRNA expression induced by these TLR agonists (Figure 2); a control RP had no effect. In A549 ECs, the effect of concurrent PAR<sub>2</sub> AP and LPS co-stimulation on IL-8 mRNA expression was additive (Figure 2a). However, in SW620 ECs, PAR<sub>2</sub> AP potentiated LPS-induced IL-8 mRNA synergistically (Figure 2b). As for PAR<sub>2</sub> and TLR2, cooperative signaling for IL-8 mRNA induction was

detected in both EC lines (Figure 2). In addition, PAR<sub>2</sub> AP, together with the TLR3 agonist, poly I:C, induced robust, synergistic augmentation of IL-8 mRNA levels in both EC lines (Figure 2).

### Cooperative and non-cooperative PAR<sub>2</sub>-TLR3 signaling integration

As the synergy between PAR<sub>2</sub> and TLR3 was the strongest observed for any of the agonist combinations tested, we examined PAR<sub>2</sub>-TLR3 signaling interactions further. Poly I:C stimulates MyD88-independent signaling by recruiting the adapter protein, TRIF, to the TLR3 dimer. Although MyD88-dependent signaling is predominantly associated with NF-κB activation, TRIF-dependent signaling results in the activation of IFN regulatory factor-3 (IRF-3) and delayed NF-κB activation (reviewed in Akira and Takeda<sup>8</sup> and Akira *et al.*<sup>9</sup>). Although NF-κB is most often associated with the induction of proinflammatory cytokines and chemokines, for example, IL-8 and MIP-3α, IRF-3 is a potent transcriptional activator of many MyD88-independent genes, including IFN-β, IP-10, and RANTES.<sup>25,26</sup> In both EC lines, PAR<sub>2</sub> AP induced mRNA expression of IL-8 and MIP-3α, but did not stimulate the expression of IFN-β, IP-10, or RANTES mRNAs (Figure 3). PAR<sub>2</sub> AP synergistically enhanced poly I:C-induced mRNA expression of IL-8 and MIP-3α (Figure 3, top panels). In contrast, PAR<sub>2</sub> AP significantly downregulated poly I:C-induced mRNA expression of IFN-β, IP-10, and RANTES (Figure 3). In A549 ECs, poly I:C-induced IFN-β mRNA expression peaked at ~2 h after stimulation (Figure 4); IP-10 mRNA expression was relatively delayed, consistent with its IFN-β dependence.<sup>25–27</sup> PAR<sub>2</sub> AP suppressed poly I:C-induced IFN-β mRNA levels significantly at 2–4 h and markedly inhibited poly I:C-induced mRNA expression of IP-10 and RANTES at 3–6 h after stimulation. In contrast, PAR<sub>2</sub> AP enhanced poly I:C-induced IL-8 and MIP-3α mRNAs at all time points examined (Figure 4). Poly I:C, but not PAR<sub>2</sub> AP, induced TLR3 mRNA expression (Figure 4),<sup>26,28</sup> and the delayed induction kinetics reflects its IFN-β dependence.<sup>26</sup> Consistent with its inhibitory effect on poly I:C-induced IFN-β gene expression, PAR<sub>2</sub> AP also inhibited poly I:C-induced TLR3 mRNA expression (Figure 4). Kinetic analysis of SW620 ECs stimulated with PAR<sub>2</sub> AP and/or poly I:C yielded similar results (data not shown). In contrast to its effects on poly I:C-induced IFN-β, IP-10, RANTES, and TLR3 mRNAs in A549 ECs, PAR<sub>2</sub> AP enhanced mRNA expression of other TLR3-driven, NF-κB-regulated genes, that is, MCP-1, MIP-2α, TNF-α, IL-6, and IL-1β (data not shown). Consistent with the mRNA data, PAR<sub>2</sub> AP augmented poly I:C-induced IL-8 and MIP-3α protein production synergistically, but suppressed poly I:C-induced IP-10 and RANTES secretion significantly in A549 ECs (Figure 5).

### PAR<sub>2</sub> AP differentially modulates TLR3-mediated activation of NF-κB and IRF-3

Consistent with the observation that the NF-κB-responsive genes, for example, IL-8 and MIP-3α, were significantly upregulated by PAR<sub>2</sub> and TLR3 co-stimulation, NF-κB p65 activation (phospho-Ser536) was enhanced in A549 ECs co-stimulated with AP and poly I:C vs. AP or poly I:C alone (Figure 6a). This observation was supported by a significant reduction in the levels of the negative regulator of NF-κB, IκBα (Figure 6b). In contrast to augmented NF-κB activation, PAR<sub>2</sub> AP downregulated poly I:C-induced IRF-3 activation (phospho-Ser396) significantly (Figure 6c). Total IRF-3 levels were unaffected (Figure 6a–c). Experiments in HEK293T cells transiently transfected with PAR<sub>2</sub>, TLR3, and luciferase reporter constructs driven by promoters having either interferon-stimulated response element (ISRE) or NF-κB binding sites showed similar results: PAR<sub>2</sub> AP co-stimulation inhibited poly I:C-induced ISRE-luciferase activity, whereas AP and poly I:C co-treatments induced higher NF-κB-luciferase reporter activity than AP or poly I:C alone (data not shown).

### PAR<sub>2</sub> AP suppresses TLR3-induced STAT1 activation

Poly I:C triggers the TLR3/IRF-3 pathway to induce the expression of IFN- $\beta$  that then binds to the type I interferon- $\alpha/\beta$  receptor (IFN- $\alpha/\beta$ R),<sup>25–27</sup> resulting in the activation of several transcription factors, including STAT1. As PAR<sub>2</sub> AP suppressed poly I:C-induced IRF-3 activation and mRNA expression of IRF-3-dependent genes, including IFN- $\beta$ , we predicted that AP would also suppress poly I:C-induced STAT1 activation. In A549 ECs, STAT1 Tyr701 phosphorylation (p-STAT1) was prominently induced at ~3 h after stimulation with poly I:C, but not with PAR<sub>2</sub> AP at any time point examined; however, AP significantly inhibited p-STAT1 levels in poly I:C-treated ECs (Figure 6d). Total STAT1 levels were unaffected. Together, these data support the finding that PAR<sub>2</sub> engagement can simultaneously augment TLR3-driven NF- $\kappa$ B activation while inhibiting TLR3-mediated IRF-3 responses, leading to downregulation of the second wave of signaling induced by the IFN- $\beta$ /IFN- $\alpha/\beta$ R/STAT1 pathway.

We next asked whether PAR<sub>2</sub> AP would also inhibit IFN- $\beta$ -induced STAT1 activation. In contrast to its inhibitory effect on poly I:C-induced STAT1 activation, PAR<sub>2</sub> AP co-stimulation did not inhibit recombinant IFN- $\beta$  (rIFN- $\beta$ )-induced p-STAT1 levels in A549 ECs (Figure 6e).

### PAR<sub>2</sub><sup>-/-</sup> and TLR4<sup>-/-</sup> mice are protected from influenza-induced lethality

As PAR<sub>2</sub> activation inhibited the TLR3/IRF-3 antiviral pathway in mucosal ECs, we hypothesized that PAR<sub>2</sub><sup>-/-</sup> mice would exhibit a de-repressed TLR3/IRF-3-mediated antiviral response and, thus, would exhibit increased protection against virus infection. Influenza A virus infection activates multiple PRRs, including MDA-5, RIG-I, and TLR3,<sup>3,4</sup> but also generates significant tissue damage that produces extracellular proteinases,<sup>5,6</sup> including elastase,<sup>5</sup> that could activate PAR<sub>2</sub> (reviewed in Vroiling *et al.*). WT C57BL/6J and PAR<sub>2</sub><sup>-/-</sup> mice were infected intranasally with mouse-adapted H1N1 influenza virus, strain A/PR/8/34. At 200 p.f.u. (plaque-forming unit), ~80% of WT mice died by day 14 after infection; in contrast, most of the PAR<sub>2</sub><sup>-/-</sup> mice survived the infection (Figure 7a). At 600 p.f.u., all mice from both strains succumbed equally (data not shown). We reasoned that if PAR<sub>2</sub><sup>-/-</sup> mice were resistant to influenza virus-induced lethality secondary to a de-repressed TLR3/IRF-3/IFN- $\beta$ -mediated antiviral response, IFN- $\beta$ <sup>-/-</sup> mice would exhibit the opposite phenotype. Although most of the PAR<sub>2</sub><sup>-/-</sup> mice survived the influenza infection (200 p.f.u.) vs. WT mice, all the IFN- $\beta$ <sup>-/-</sup> mice died (Figure 7b). Taken together, these *in vivo* data support our observations in EC lines that PAR<sub>2</sub> activation inhibits the antiviral response induced by innate immune biosensors, such as TLR3. The absence of PAR<sub>2</sub> conferred a protective phenotype on influenza-infected mice.

Previously, we showed receptor cooperativity between PAR<sub>2</sub> and TLR4 *in vitro*.<sup>23</sup> In HEK293T transfectants, PAR<sub>2</sub> engagement by its AP resulted in NF- $\kappa$ B activation that was synergistically enhanced by the coexpression of TLR4. TLR4-mediated enhancement of PAR<sub>2</sub> signaling was MyD88-dependent, whereas PAR<sub>2</sub> signaling in the absence of TLR4 was TRIF dependent.<sup>23</sup> Conversely, PAR<sub>2</sub> AP-treated TLR4<sup>-/-</sup> macrophages exhibited significantly diminished expression of NF- $\kappa$ B-dependent IL-1 $\beta$  mRNA vs. WT macrophages. In the HEK293T transfection system, PAR<sub>2</sub> AP induced a physical association between PAR<sub>2</sub> and TLR4.<sup>23</sup> We concluded from our earlier study that optimal PAR<sub>2</sub> signaling leading to NF- $\kappa$ B activation occurs when in complex with TLR4 and its adapter protein, MyD88.<sup>23</sup>

Given that optimal PAR<sub>2</sub> signaling requires TLR4,<sup>23</sup> and as PAR<sub>2</sub><sup>-/-</sup> mice were resistant to influenza-induced lethality, we hypothesized that TLR4<sup>-/-</sup> mice would be similarly protected. Similar to PAR<sub>2</sub><sup>-/-</sup> mice, most of the TLR4<sup>-/-</sup> mice survived H1N1 influenza A virus infection, under conditions in which most of the WT mice died (Figure 7c).

### TLR4 contributes to PAR<sub>2</sub>-mediated inflammation *in vivo*

To test further the hypothesis that PAR<sub>2</sub>-TLR4 receptor cooperativity occurs *in vivo*, we also used a well-characterized footpad edema model.<sup>29</sup> Injection of PAR<sub>2</sub> AP, but not saline or an inactive, control (reverse) peptide (RP), into the hind footpads of WT C57BL/6J mice rapidly induced edema that peaked at 1 h (Figure 8). Neither PAR<sub>2</sub> AP nor RP induced footpad edema in PAR<sub>2</sub><sup>-/-</sup> mice (Figure 8a). Compared to the WT response, PAR<sub>2</sub> AP-induced footpad edema was significantly diminished in both TLR4<sup>-/-</sup> and MyD88<sup>-/-</sup> mice (Figure 8a and b). Together, these *in vivo* data further support our recently described novel model of PAR<sub>2</sub>-TLR4 receptor cooperativity<sup>23</sup> in which optimal PAR<sub>2</sub> signaling leading to an inflammatory response requires TLR4 and MyD88.

## DISCUSSION

Signaling pathways coordinately triggered by distinct innate immune PRRs on activation by microbial components, for example, PAMPs, proteinases, have the potential to synergize with or antagonize one another to modulate an inflammatory response to infection. Results from our recent study showed that PAR<sub>2</sub> and TLR4 synergized *in vitro* to augment a MyD88-mediated, NF-κB-dependent inflammatory response.<sup>23</sup> In this study, we have extended these original observations by studying signaling interactions between the classical PRRs, that is, TLR2, TLR3, and TLR4, and a nonclassical PRR, that is, PAR<sub>2</sub>, in A549 and SW620 ECs derived from human respiratory and colonic mucosa, respectively. Our data presented herein support the conclusion that PAR<sub>2</sub>-TLR signaling integration drives “customized” inflammatory responses to combinatorial “danger” stimuli from the environment. We observed cooperative signaling convergence between PAR<sub>2</sub> and TLR2, TLR3, or TLR4 for mRNA induction of NF-κB-dependent IL-8, a potent neutrophil chemoattractant; cooperation between PAR<sub>2</sub> and TLR3 was highly synergistic. We also showed, for the first time, that PAR<sub>2</sub> coactivation led to differential signaling outcomes in TLR3-stimulated mucosal ECs. We revealed a novel role for PAR<sub>2</sub> in the negative regulation of TLR/IRF-3 antiviral pathway, leading to reduced expression of TLR3-, IRF-3-driven genes, for example, IFN-β, IP-10, and RANTES. Mechanistically, these PAR<sub>2</sub>-mediated differential effects on TLR3 signaling were traced to changes in the level of activation of the transcription factors, NF-κB and IRF-3. The inhibitory effect of PAR<sub>2</sub> AP on TLR3-driven IRF-3 activation resulted in reduced IFN-β expression and significant suppression of TLR3-inducible STAT1 activation. These *in vitro* observations in EC lines were supported by results showing that PAR<sub>2</sub><sup>-/-</sup> mice were more resistant to lethality following intranasal infection with H1N1 influenza A virus than WT C57BL/6J mice, whereas IFN-β<sup>-/-</sup> mice were hypersusceptible.

During viral infection, RNA from viruses can be sensed by TLRs 3, 7, and 8, as well as the RNA helicase cytosolic sensors, RIG-I and MDA-5 (reviewed in Kawai and Akira<sup>30</sup>). We examined the cellular responses to TLR3 stimulation as a representative TLR-dependent antiviral pathway in mucosal ECs. Ligand-bound TLR3 activates several transcription factors, including IRF-3 and NF-κB.<sup>31</sup> Ligand-activated TLR3 dimerizes, binds its sole adapter, TRIF, and recruits IκB kinase ε (IKKε) and TANK-binding kinase 1 (TBK1).<sup>32</sup> In turn, IKKε/TBK1 activates IRF-3 through C-terminal phosphorylation. The TLR3-TRIF complex also recruits receptor-interacting protein 1 (RIP1) to couple signaling to the IKKα/β/γ complex for NF-κB activation.<sup>33</sup> Although activated NF-κB translocates to the nucleus and induces transcription of many proinflammatory cytokine or chemokine genes, for example, IL-8, MIP-3α, phosphorylated IRF-3 homodimers translocate to the nucleus to induce transcription of type I IFNs and many other IRF-3-regulated genes, for example, IFN-β, IP-10, and RANTES.<sup>34</sup> Induction of type I IFNs is critical for evoking the expression of additional antiviral genes through the IFN-α/βR/STAT1 signaling pathway.<sup>25–27</sup>

Both IRF-3 and NF- $\kappa$ B are required for transcriptional activation of the potent antiviral protein, IFN- $\beta$  (reviewed in Kawai and Akira<sup>30</sup>). Although PAR<sub>2</sub> AP enhanced poly I:C-induced NF- $\kappa$ B activation, AP markedly inhibited poly I:C-driven IRF-3 activation, consistent with AP-mediated suppression of TLR3-driven IFN- $\beta$  mRNA expression. The inhibitory effect of AP on the TLR3/IRF-3 signaling pathway appears to be very early, at the level of IKK $\epsilon$ /TBK1 phosphorylation of IRF-3, rather than a result of altered IRF-3 protein stability. This is further supported by the observation that poly I:C-induced, but not rIFN- $\beta$ -induced, phosphorylation of STAT1 was inhibited by concurrent stimulation of PAR<sub>2</sub> by AP. The LPS-transducing receptor, TLR4, is the only other TLR that signals through the TRIF/IKK $\epsilon$ /TBK1/IRF-3 pathway (reviewed in Akira and Takeda<sup>8</sup>). In SW620 ECs, LPS-induced expression of IFN- $\beta$  and IP-10 mRNAs was attenuated significantly by PAR<sub>2</sub> AP co-stimulation (Supplementary Figure S1a online). In A549 ECs, PAR<sub>2</sub> AP co-stimulation also inhibited LPS-induced IP-10 mRNA expression significantly (Supplementary Figure S1b). Taken together, these data suggest that PAR<sub>2</sub> activation exerts a more generalized inhibitory effect on the TLR/TRIF, that is, TLR3/TRIF and TLR4/TRIF, signaling pathway.

Consistent with previous reports attributing a positive, cooperative signaling outcome between PAR<sub>2</sub> and TLRs,<sup>22–24</sup> we showed positive cooperativity between PAR<sub>2</sub> and TLRs at the level of NF- $\kappa$ B activation. The cooperative convergence of NF- $\kappa$ B signaling derived from these two distinct PRR families supports our contention of their proposed roles as biosensors of infection. Enhanced NF- $\kappa$ B activation is predicted to be critical for optimal induction of inflammatory mediators, including the expression of chemokines and cytokines necessary for the recruitment and activation of circulating leukocytes to the nidus of infection. However, selective augmentation and suppression of cytokine/chemokine expression likely has an important role in the pathogenesis and persistence/clearance of a given infection. That PAR<sub>2</sub> activation augmented TLR3-driven expression of some chemokines, for example, IL-8 and MIP-3 $\alpha$ , yet suppressed the expression of others, for example, IP-10 and RANTES, suggests that proteinase-rich microenvironments might drastically alter the composition of infiltrating leukocytes and, thus, significantly alter the inflammatory outcome of an infection.

Under physiological conditions, extracellular proteinases are tightly regulated by many mechanisms, including the regulation of proteinase expression and their negative control by anti-proteinases. Reduced expression of anti-proteinases and/or enhanced local levels of pathogen-and/or host-derived proteinases can lead to a dysregulated proteinase/anti-proteinase balance at anatomical sites where extracellular proteolysis is undesirable (reviewed in Antalis *et al.*<sup>35</sup>). Given that PAR<sub>2</sub> activation negatively regulated the TLR3/IRF-3 antiviral pathway, we speculated that in tissues in which both PAR<sub>2</sub> and TLR3 are present, for example, the airway, disease processes with dysregulated and de-repressed extracellular PAR<sub>2</sub>-activating trypsin-like proteolytic activities might be more susceptible to infection with TLR3-triggering viruses such as influenza A.<sup>3,4</sup> We confirmed this hypothesis by infecting WT C57BL/6J and PAR<sub>2</sub><sup>-/-</sup> mice with mouse-adapted H1N1 influenza A virus that can activate TLR3 and also generates extracellular proteinases that can trigger PAR<sub>2</sub>. In support of our *in vitro* observations in EC cultures, in three separate experiments, PAR<sub>2</sub><sup>-/-</sup> mice were protected from challenge with influenza A virus. In contrast, IFN- $\beta$ <sup>-/-</sup> mice were hypersusceptible to influenza virus-induced lethality. Taken together, both the *in vitro* and *in vivo* data support our model that PAR<sub>2</sub> activation inhibits TLR/IRF-3 antiviral pathway; the absence of PAR<sub>2</sub> conferred a protective phenotype in influenza-infected mice. The absence of PAR<sub>2</sub> might also mitigate the NF- $\kappa$ B-mediated cytokine storm induced by influenza infection leading, in part, to the resistance of PAR<sub>2</sub><sup>-/-</sup> mice to influenza-induced lethality.

In contrast to our findings using 200 p.f.u. influenza virus per mouse, Khoufache *et al.*<sup>36</sup> recently reported that PAR<sub>2</sub><sup>-/-</sup> mice were more susceptible to intranasal infection with cell culture-propagated H1N1 influenza A/PR/8/34 virus (30–60 p.f.u. per mouse). Differences in

infectious dose, method of virus propagation (i.e., cell culture vs. allantoic fluid of embryonated eggs), and housing conditions may account for the discrepancies between results reported by us and Khoufache *et al.* and warrant further investigation. It is unlikely, though, that our viral dose (200 p.f.u.) was less infectious because it killed ~80% of the WT mice, whereas their dose of 30–60 p.f.u. was nonlethal in PAR<sub>2</sub><sup>+/+</sup> mice. However, we hypothesize that different infectious doses used in the two studies (200 p.f.u. vs. 30–60 p.f.u.) perhaps led to differential levels of PAR<sub>2</sub> receptor expression or activation that could potentially account for the opposite findings. The extent of tissue damage, the level of PAR<sub>2</sub>-activating enzymes generated, and the degree of PAR<sub>2</sub> receptor activation secondary to influenza infection are likely to be different at the two viral doses. In support of this hypothesis, it has been shown that differential stimulus dosage, for example, low vs. high agonist concentrations, can result in opposite biological effects. For example, Eisenbarth *et al.*<sup>37</sup> showed that low levels of LPS induced T-helper cell type 2 responses to an inhaled antigen, whereas high levels of inhaled LPS with the same antigen resulted in strong Th1 responses. The genetic backgrounds of the PAR<sub>2</sub><sup>-/-</sup> mice used in the two studies were also different. The different gene-targeted deletion approaches used to generate PAR<sub>2</sub><sup>-/-</sup> mice and the extent of genetic backcross may also have contributed to the opposite observations.<sup>38,39</sup> In addition, PAR<sub>2</sub> activation has been reported to exhibit opposite effects in other host inflammatory responses,<sup>40–43</sup> and perhaps this is attributable to the balance of synergistic or antagonistic effects reported herein between PAR<sub>2</sub> and activation of other PRRs by PAMPs that are concurrently present in the environment. Future studies will be necessary to determine how differences in experimental designs might have contributed to the different findings. Nevertheless, like PAR<sub>2</sub><sup>-/-</sup> mice, we observed that TLR4<sup>-/-</sup> mice were similarly protected from H1N1 influenza A virus infection, findings that are consistent with our recently described model of PAR<sub>2</sub>-TLR4 receptor cooperativity. Moreover, PAR<sub>2</sub> AP induced footpad edema in WT C57BL/6J mice that was absent in PAR<sub>2</sub><sup>-/-</sup> mice and significantly diminished in both TLR4<sup>-/-</sup> and MyD88<sup>-/-</sup> mice. We also observed significantly diminished secretion of KC and MIP-2α chemokines by TLR4<sup>-/-</sup> vs. WT C57BL/6J colonic intestinal tissues cultured *ex vivo* and treated with PAR<sub>2</sub> AP (data not shown). Moretti *et al.*<sup>18</sup> reported recently that PAR<sub>2</sub> signaling in murine polymorphonuclear neutrophils depended on the presence of TLR4.

Interference of host innate antiviral defense by influenza virus is known to be achieved by the nonstructural NS1 viral protein, which dampens the induction of IRF-3-responsive antiviral genes, including IFN-β.<sup>44</sup> However, infection of host cells by orthomyxoviruses and paramyxoviruses can also be enhanced by host/pathogen-derived proteinases<sup>45</sup> (and reviewed in Kido *et al.*<sup>46</sup>). For example, co-infection with *Staphylococcus aureus* strains that secrete trypsin-like serine proteinases enhances influenza virus infectivity significantly by mediating cleavage of viral fusion glycoproteins, for example, hemagglutinin.<sup>45</sup> In this study, we have provided evidence for an additional mechanism by which host/pathogen-derived proteinases might diminish TLR-mediated host antiviral response through the activation of PAR<sub>2</sub>. It is tempting to speculate that natural selection and host-virus co-evolution led to the utilization of proteinases for enhanced virus infectivity by simultaneously facilitating host-virus membrane fusion and interfering with host antiviral defense.

In summary, results from this study provide compelling data that suggest that regulating the extracellular proteinase/anti-proteinase balance might represent an effective therapeutic approach to controlling orthomyxovirus and paramyxovirus infections. The results from this study also represent a novel example of cooperative and non-cooperative signaling integration between heterologous PRRs of the innate immune system.



## METHODS

### Reagents, virus, cell culture, and mice

Human PAR<sub>2</sub> AP, SLIGKV-NH<sub>2</sub>, and an inactive control RP, VKGILS-NH<sub>2</sub>, were synthesized (>96% purity) by Phoenix Pharmaceuticals (Belmont, CA). Protein-free, phenol/water extracted LPS from *Escherichia coli* strain K235 was purified as referenced.<sup>23</sup> S-[2,3-bis (palmitoyloxy)-(2-RS)-propyl]-[R]-Cys-Ser-Lys<sub>4</sub>-OH (Pam2CSK4 or P2C) and poly I:C (pI:C) were purchased from Invivogen (San Diego, CA). Human rIFN- $\beta$  1a was purchased from PBL InterferonSource (Piscataway, NJ). Mouse-adapted H1N1 influenza virus (A/PR/8/34) was purchased from American Type Culture Collection (ATCC) (Manassas, VA) and grown in the allantoic fluid of 10-day old embryonated chicken eggs (Charles River Laboratories, Wilmington, MA) as previously described.<sup>47</sup> Human A549 lung and SW620 colonic ECs (ATCC) were propagated in Dulbecco's modified Eagle's medium (DMEM) or RPMI-1640 (CellGro, Herndon, VA), respectively. DMEM was supplemented with 10% heat-inactivated fetal calf serum (FCS; Hyclone, Logan, UT), 100 U ml<sup>-1</sup> penicillin, 100  $\mu$ g ml<sup>-1</sup> streptomycin, and 2 mM L-glutamine. RPMI-1640 received the same supplements, but with 2% heat-inactivated FCS. ECs were harvested from tissue culture flasks (Corning, Corning, NY) using CellStripper solution (CellGro) and seeded in 6-well plates at 4 $\times$ 10<sup>5</sup> (A549) or 1 $\times$ 10<sup>6</sup> (SW620) cells per well. Cells were allowed to rest for 2 days with a medium change on day 1, and treated with agonists, as indicated. WT C57BL/6J mice and PAR<sub>2</sub><sup>-/-</sup> mice backcrossed onto a C57BL/6 background (N5) were purchased from The Jackson Laboratories (Bar Harbor, ME). TLR4<sup>-/-</sup> and MyD88<sup>-/-</sup> mice (N $\geq$ 8 on a C57BL/6 background), originally obtained from Dr Shizuo Akira (Osaka University, Osaka, Japan), and IFN- $\beta$ <sup>-/-</sup> mice (N $\geq$ 8 on a C57BL/6 background), originally obtained from Dr Eleanor Fish (University of Toronto, Ontario, Canada), were bred at UMB. Mice were housed in a SPF barrier facility (UMB). Administration of AP or influenza to mice is described in the figure legends. All mice were age matched and used between 6–10 weeks of age. All experiments were conducted with institutional approval.

### Preparation of total RNA and cDNA

Total RNA from EC cultures was extracted, and oligo(dT)-primed cDNA was synthesized as previously described.<sup>28</sup>

### qPCR

Quantitative real-time PCR (qPCR) primers (Table 1) were designed and synthesized as previously described.<sup>28</sup> qPCR was carried out on ABI Prism 7500 Fast Real-time PCR System (Applied Biosystems, Foster City, CA) in a 25  $\mu$ l reaction containing 20 ng cDNA, 0.3  $\mu$ M each of sense/anti-sense primers, and 12.5  $\mu$ l of Fast SYBR Green Master Mix (Applied Biosystems) under the manufacturer's pre-set thermal conditions: 20 s at 95 °C, 40 cycles of 3 s at 95 °C and 30 s at 60 °C, followed by a dissociation stage. Relative gene expression was calculated using the 2<sup>- $\Delta\Delta$ Ct</sup> method as previously referenced,<sup>28</sup> with hypoxanthine guanine phosphoribosyltransferase as the housekeeping gene.

### Western analysis

A549 cells were seeded at 8 $\times$ 10<sup>5</sup> cells per well in 6-well plates and allowed to rest for 3 days, with a medium change on day 1. After treatment, whole-cell lysates were collected, processed, resolved by gel electrophoresis, transferred to polyvinylidene difluoride membranes, probed with antibodies, and target protein bands detected as previously described.<sup>28</sup> Primary and horseradish peroxidase-conjugated secondary antibodies used in this study were purchased from Cell Signaling Technology (Danvers, MA) and used at 1:1,000 and 1:2,000 dilutions, respectively.

## Analysis of secreted proteins by ELISA

The concentrations of secreted proteins were determined by enzyme-linked immunosorbent assay (ELISA) by the Cytokine Core Laboratory (UMB).

## Statistical analysis

Using GraphPad PRISM 4.0 (GraphPad Software, San Diego, CA), oneway analysis of variance (ANOVA) with Tukey's post-test or two-way ANOVA with Bonferroni post-test was performed to assess statistical significance ( $P$ -values < 0.05).

## Supplementary Material

Refer to Web version on PubMed Central for supplementary material.

## Acknowledgments

The authors thank Ms Rachel Griffin for breeding TLR4<sup>-/-</sup>, MyD88<sup>-/-</sup>, and IFN- $\beta$ <sup>-/-</sup> mice, and Dr Prasad Rallabhandi for helpful discussion. This work was supported by the NIH Grants R37 AI-18797 (SNV), R01 DK048373 (AF), R01 HL084387, R01 DK081376, R01 CA098369 (TA), and R01 AI050632 (DF). QMN was supported, in part, by the NIH Training Grant (T32 AI-07540) and is currently supported by AI-18797 (SNV). JRT was supported by a minority supplement R01 AI050632S1. This work was carried out in partial fulfillment of the PhD requirements (QMN).

## REFERENCES

- Gribar SC, Richardson WM, Sodhi CP, Hackam DJ. No longer an innocent bystander: epithelial Toll-like receptor signaling in the development of mucosal inflammation. *Mol. Med* 2008;14:645–659. [PubMed: 18584047]
- Vroeling AB, Fokkens WJ, Van Drunen CM. How epithelial cells detect danger: aiding the immune response. *Allergy* 2008;63:1110–1123. [PubMed: 18699929]
- Le Goffic R, et al. Cutting Edge: Influenza A virus activates TLR3-dependent inflammatory and RIG-I-dependent antiviral responses in human lung epithelial cells. *J. Immunol* 2007;178:3368–3372. [PubMed: 17339430]
- Le Goffic R, et al. Detrimental contribution of the Toll-like receptor (TLR)3 to influenza A virus-induced acute pneumonia. *PLoS Pathog* 2006;2:e53. [PubMed: 16789835]
- Buchweitz JP, Harkema JR, Kaminski NE. Time-dependent airway epithelial and inflammatory cell responses induced by influenza virus A/PR/8/34 in C57BL/6 mice. *Toxicol. Pathol* 2007;35:424–435. [PubMed: 17487773]
- Serkedjieva J, Toshkova R, Antonova-Nikolova S, Stefanova T, Teodosieva A, Ivanova I. Effect of a plant polyphenol-rich extract on the lung protease activities of influenza-virus-infected mice. *Antivir. Chem. Chemother* 2007;18:75–82. [PubMed: 17542152]
- Janeway CA Jr, Medzhitov R. Innate immune recognition. *Annu. Rev. Immunol* 2002;20:197–216. [PubMed: 11861602]
- Akira S, Takeda K. Toll-like receptor signalling. *Nat. Rev. Immunol* 2004;4:499–511. [PubMed: 15229469]
- Akira S, Uematsu S, Takeuchi O. Pathogen recognition and innate immunity. *Cell* 2006;124:783–801. [PubMed: 16497588]
- Steinhoff M, et al. Proteinase-activated receptors: transducers of proteinase-mediated signaling in inflammation and immune response. *Endocr. Rev* 2005;26:1–43. [PubMed: 15689571]
- Ramachandran R, Hollenberg MD. Proteinases and signalling: pathophysiological and therapeutic implications via PARs and more. *Br. J. Pharmacol* 2008;153:S263–S282. [PubMed: 18059329]
- Sun G, Stacey MA, Schmidt M, Mori L, Mattoli S. Interaction of mite allergens Der p3 and Der p9 with protease-activated receptor-2 expressed by lung epithelial cells. *J. Immunol* 2001;167:1014–1021. [PubMed: 11441110]
- Chung WO, Hansen SR, Rao D, Dale BA. Protease-activated receptor signaling increases epithelial antimicrobial peptide expression. *J. Immunol* 2004;173:5165–5170. [PubMed: 15470061]

14. Kida Y, Inoue H, Shimizu T, Kuwano K. *Serratia marcescens* serralyisin induces inflammatory responses through protease-activated receptor 2. *Infect. Immun* 2007;75:164–174. [PubMed: 17043106]
15. Dommissch H, et al. Protease-activated receptor 2 mediates human beta-defensin 2 and CC chemokine ligand 20 mRNA expression in response to proteases secreted by *Porphyromonas gingivalis*. *Infect. Immun* 2007;75:4326–4333. [PubMed: 17591792]
16. Moraes TJ, et al. Role of PAR2 in murine pulmonary pseudomonal infection. *Am. J. Physiol. Lung Cell. Mol. Physiol* 2008;294:L368–L377. [PubMed: 18083764]
17. Devlin MG, Gasser RB, Cocks TM. Initial support for the hypothesis that PAR<sub>2</sub> is involved in the immune response to *Nippostrongylus brasiliensis* in mice. *Parasitol. Res* 2007;101:105–109. [PubMed: 17458579]
18. Moretti S, et al. The contribution of PARs to inflammation and immunity to fungi. *Mucosal Immunol* 2008;1:156–168. [PubMed: 19079173]
19. Trinchieri G, Sher A. Cooperation of Toll-like receptor signals in innate immune defence. *Nat. Rev. Immunol* 2007;7:179–190. [PubMed: 17318230]
20. O'Neill LA. When signaling pathways collide: positive and negative regulation of Toll-like receptor signal transduction. *Immunity* 2008;29:12–20. [PubMed: 18631453]
21. Fyfe M, Bergstrom M, Aspengren S, Peterson A. PAR-2 activation in intestinal epithelial cells potentiates interleukin-1 $\beta$ -induced chemokine secretion via MAP kinase signaling pathways. *Cytokine* 2005;31:358–367. [PubMed: 16095910]
22. Ostrowska E, Sokolova E, Reiser G. PAR-2 activation and LPS synergistically enhance inflammatory signaling in airway epithelial cells by raising PAR expression level and interleukin-8 release. *Am. J. Physiol. Lung Cell. Mol. Physiol* 2007;293:L1208–L1218. [PubMed: 17766588]
23. Rallabhandi P, et al. Analysis of proteinase-activated receptor 2 and TLR4 signal transduction: a novel paradigm for receptor cooperativity. *J. Biol. Chem* 2008;283:24314–24325. [PubMed: 18622013]
24. Uehara A, Hirabayashi Y, Takada H. Antibodies to proteinase 3 prime human oral, lung, and kidney epithelial cells to secrete proinflammatory cytokines upon stimulation with agonists to various Toll-like receptors, NOD1, and NOD2. *Clin. Vaccine Immunol* 2008;15:1060–1066. [PubMed: 18495849]
25. Doyle S, et al. IRF3 mediates a TLR3/TLR4-specific antiviral gene program. *Immunity* 2002;17:251–263. [PubMed: 12354379]
26. Doyle SE, O'Connell R, Vaidya SA, Chowoyle EK, Yee K, Cheng G. Toll-like receptor 3 mediates a more potent antiviral response than Toll-like receptor 4. *J. Immunol* 2003;170:3565–3571. [PubMed: 12646618]
27. Toshchakov V, et al. TLR4, but not TLR2, mediates IFN- $\beta$ -induced STAT1 $\alpha$ / $\beta$ -dependent gene expression in macrophages. *Nat. Immunol* 2002;3:392–398. [PubMed: 11896392]
28. Nhu QM, Cuesta N, Vogel SN. Transcriptional regulation of lipopolysaccharide (LPS)-induced Toll-like receptor (TLR) expression in murine macrophages: role of interferon regulatory factors 1 (IRF-1) and 2 (IRF-2). *J. Endotoxin Res* 2006;12:285–295. [PubMed: 17059692]
29. Vergnolle N, Hollenberg MD, Sharkey KA, Wallace JL. Characterization of the inflammatory response to proteinase-activated receptor-2 (PAR2)-activating peptides in the rat paw. *Br. J. Pharmacol* 1999;127:1083–1090. [PubMed: 10455252]
30. Kawai T, Akira S. Innate immune recognition of viral infection. *Nat. Immunol* 2006;7:131–137. [PubMed: 16424890]
31. Jiang Z, Mak TW, Sen G, Li X. Toll-like receptor 3-mediated activation of NF- $\kappa$ B and IRF3 diverges at Toll-IL-1 receptor domain-containing adapter inducing IFN- $\beta$ . *Proc. Natl. Acad. Sci. USA* 2004;101:3533–3538. [PubMed: 14982987]
32. Fitzgerald KA, et al. IKK $\epsilon$  and TBK1 are essential components of the IRF3 signaling pathway. *Nat. Immunol* 2003;4:491–496. [PubMed: 12692549]
33. Meylan E, et al. RIP1 is an essential mediator of Toll-like receptor 3-induced NF- $\kappa$ B activation. *Nat. Immunol* 2004;5:503–507. [PubMed: 15064760]

34. Yoneyama M, Suhara W, Fukuhara Y, Fukuda M, Nishida E, Fujita T. Direct triggering of the type I interferon system by virus infection: activation of a transcription factor complex containing IRF-3 and CBP/p300. *EMBO J* 1998;17:1087–1095. [PubMed: 9463386]
35. Antalis TM, Shea-Donohue T, Vogel SN, Sears C, Fasano A. Mechanisms of disease: protease functions in intestinal mucosal pathobiology. *Nat. Clin. Pract. Gastroenterol. Hepatol* 2007;4:393–402. [PubMed: 17607295]
36. Khoufache K, et al. Protective role for protease-activated receptor-2 against influenza virus pathogenesis via an IFN- $\gamma$ -dependent pathway. *J. Immunol* 2009;182:7795–7802. [PubMed: 19494303]
37. Eisenbarth SC, Piggott DA, Huleatt JW, Visintin I, Herrick CA, Bottomly K. Lipopolysaccharide-enhanced, toll-like receptor 4-dependent T helper cell type 2 responses to inhaled antigen. *J. Exp. Med* 2002;196:1645–1651. [PubMed: 12486107]
38. Damiano BP, et al. Cardiovascular responses mediated by protease-activated receptor-2 (PAR-2) and thrombin receptor (PAR-1) are distinguished in mice deficient in PAR-2 or PAR-1. *J. Pharmacol. Exp. Ther* 1999;288:671–678. [PubMed: 9918574]
39. Schmidlin F, et al. Protease-activated receptor 2 mediates eosinophil infiltration and hyperreactivity in allergic inflammation of the airway. *J. Immunol* 2002;169:5315–5321. [PubMed: 12391252]
40. Kawabata A, et al. The protease-activated receptor-2 agonist induces gastric mucus secretion and mucosal cytoprotection. *J. Clin. Invest* 2001;107:1443–1450. [PubMed: 11390426]
41. Cenac N, et al. Induction of intestinal inflammation in mouse by activation of proteinase-activated receptor-2. *Am. J. Pathol* 2002;161:1903–1915. [PubMed: 12414536]
42. Afkhami-Goli A, et al. Proteinase-activated receptor-2 exerts protective and pathogenic cell type-specific effects in Alzheimer's disease. *J. Immunol* 2007;179:5493–5503. [PubMed: 17911636]
43. Laukkarinen JM, Weiss ER, van Acker GJ, Steer ML, Perides G. Protease-activated receptor-2 exerts contrasting model-specific effects on acute experimental pancreatitis. *J. Biol. Chem* 2008;283:20703–20712. [PubMed: 18511423]
44. Geiss GK, et al. Cellular transcriptional profiling in influenza A virus-infected lung epithelial cells: the role of the nonstructural NS1 protein in the evasion of the host innate defense and its potential contribution to pandemic influenza. *Proc. Natl. Acad. Sci. USA* 2002;99:10736–10741. [PubMed: 12149435]
45. Tashiro M, Ciborowski P, Klenk HD, Pulverer G, Rott R. Role of *Staphylococcus* protease in the development of influenza pneumonia. *Nature* 1987;325:536–537. [PubMed: 3543690]
46. Kido H, Murakami M, Oba K, Chen Y, Towatari T. Cellular proteinases trigger the infectivity of the influenza A and Sendai viruses. *Mol. Cells* 1999;9:235–244. [PubMed: 10420980]
47. Teijaro JR, et al. Costimulation modulation uncouples protection from immunopathology in memory T cell responses to influenza virus. *J. Immunol* 2009;182:6834–6843. [PubMed: 19454679]

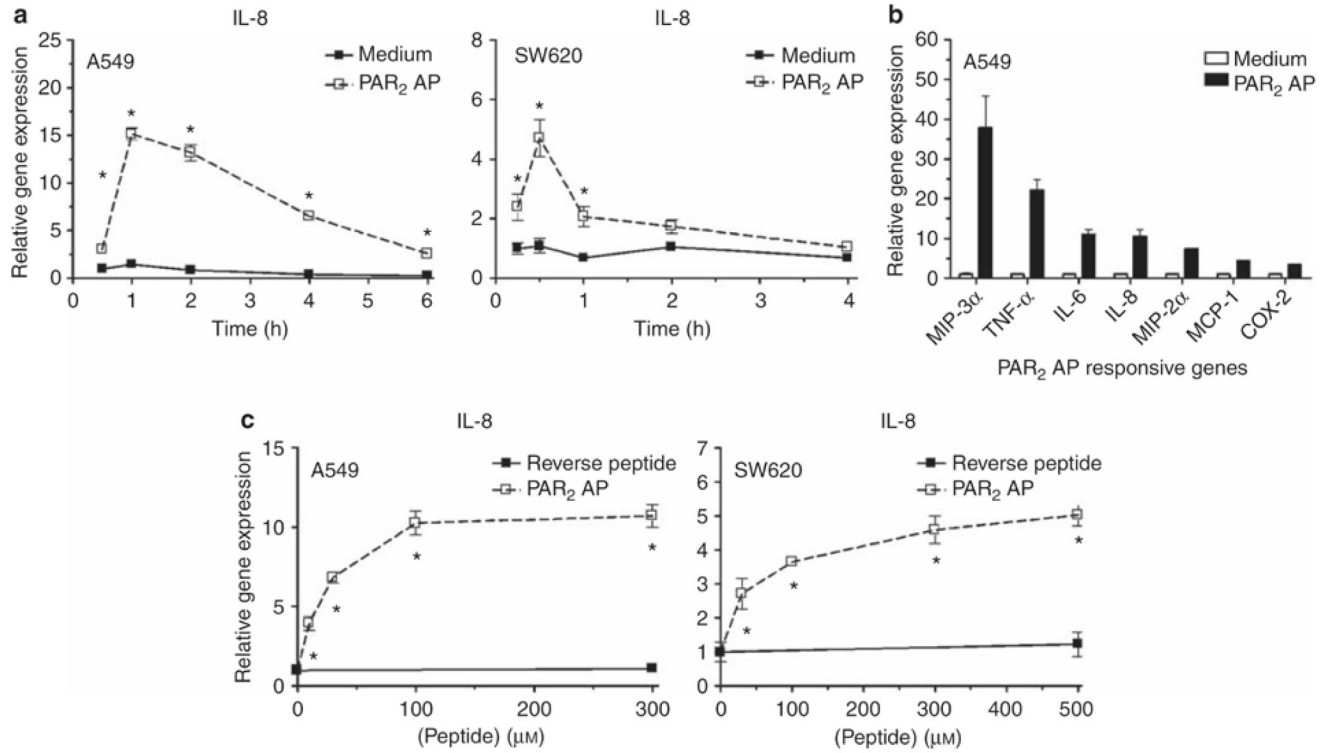


**Figure 1.** Responsiveness of human mucosal epithelial cell lines to proteinase-activated receptor 2 (PAR<sub>2</sub>) agonist peptide (AP) stimulation. **(a)** PAR<sub>2</sub> AP time course. Relative gene expression was analyzed by quantitative real-time PCR (qPCR). A549 cells were treated with medium or PAR<sub>2</sub> AP (100 μM) over the indicated time points. Data are presented as the mean ± s.d., representative of four separate experiments. SW620 cells were treated with medium or PAR<sub>2</sub> AP (300 μM) over the indicated time points. Data are presented as the mean ± s.e.m. of four separate experiments. **(b)** Inflammatory mediator genes induced in PAR<sub>2</sub> AP-treated A549 cells. A549 cells were treated with medium or PAR<sub>2</sub> AP (100 μM). Peak induction of genes examined occurred within 1–2 h after stimulation and is presented as the mean ± s.e.m. (*n*=2–6 separate experiments). **(c)** PAR<sub>2</sub> AP concentration-response curves. A549 and SW620 cells were stimulated with PAR<sub>2</sub> reverse-control peptide (300 or 500 μM, respectively) or the indicated concentrations of PAR<sub>2</sub> AP for 1 h or 30 min, respectively. Relative gene expression is presented as the mean ± s.e.m. of two separate experiments for each cell line. \* *p*<0.05.

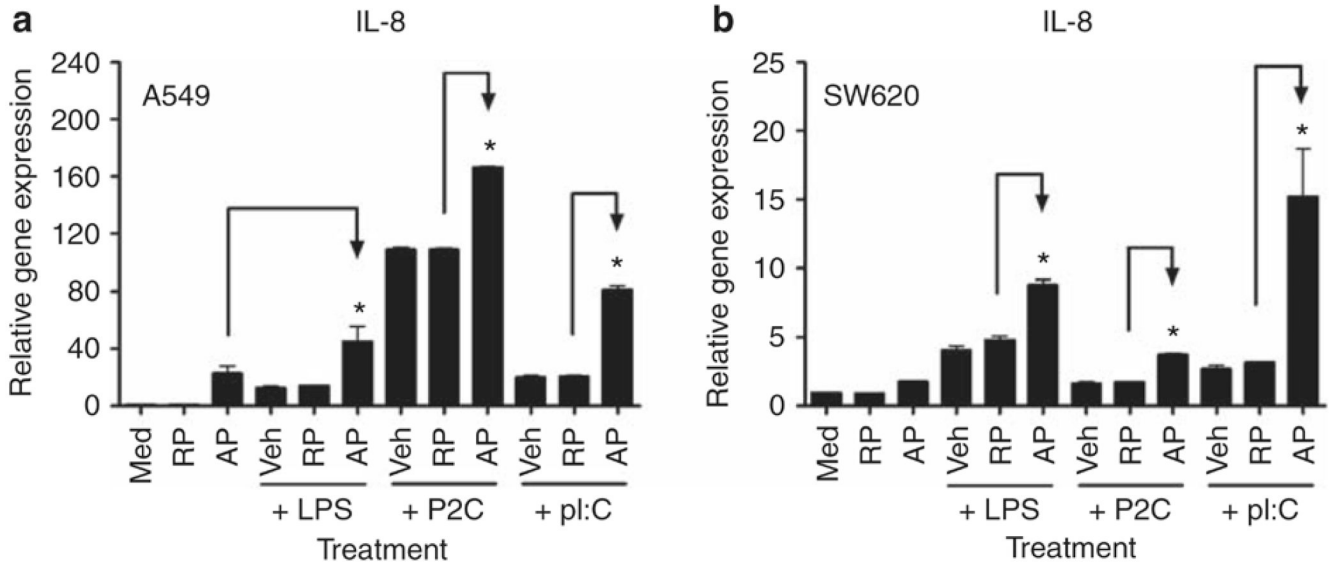


**Figure 2.** Proteinase-activated receptor 2 (PAR<sub>2</sub>) agonist peptide (AP) augments Toll-like receptor (TLR)-induced interleukin-8 (IL-8) mRNA expression in human mucosal epithelial cell lines. Relative gene expression was analyzed by quantitative real-time PCR (qPCR). **(a)** A549 cells were treated with medium (Med), PAR<sub>2</sub> reverse-control peptide (RP), or PAR<sub>2</sub> AP (100 μM), in the absence or presence of lipopolysaccharide (LPS) (1 μg ml<sup>-1</sup>), P2C (0.1 μg ml<sup>-1</sup>), or poly I:C (pI:C; 100 μg ml<sup>-1</sup>) for 3 h. Data are presented as the mean ± s.d., representative of three separate experiments. **(b)** SW620 cells were treated with medium (Med), PAR<sub>2</sub> RP, or PAR<sub>2</sub> AP (300 μM), in the absence or presence of LPS (0.1 μg ml<sup>-1</sup>), P2C (0.1 μg ml<sup>-1</sup>), or poly I:C (pI:C; 100 μg ml<sup>-1</sup>) for 3 h. Data are presented as the mean ± s.d., representative of three separate experiments. Veh, vehicle; \* *p*<0.05.

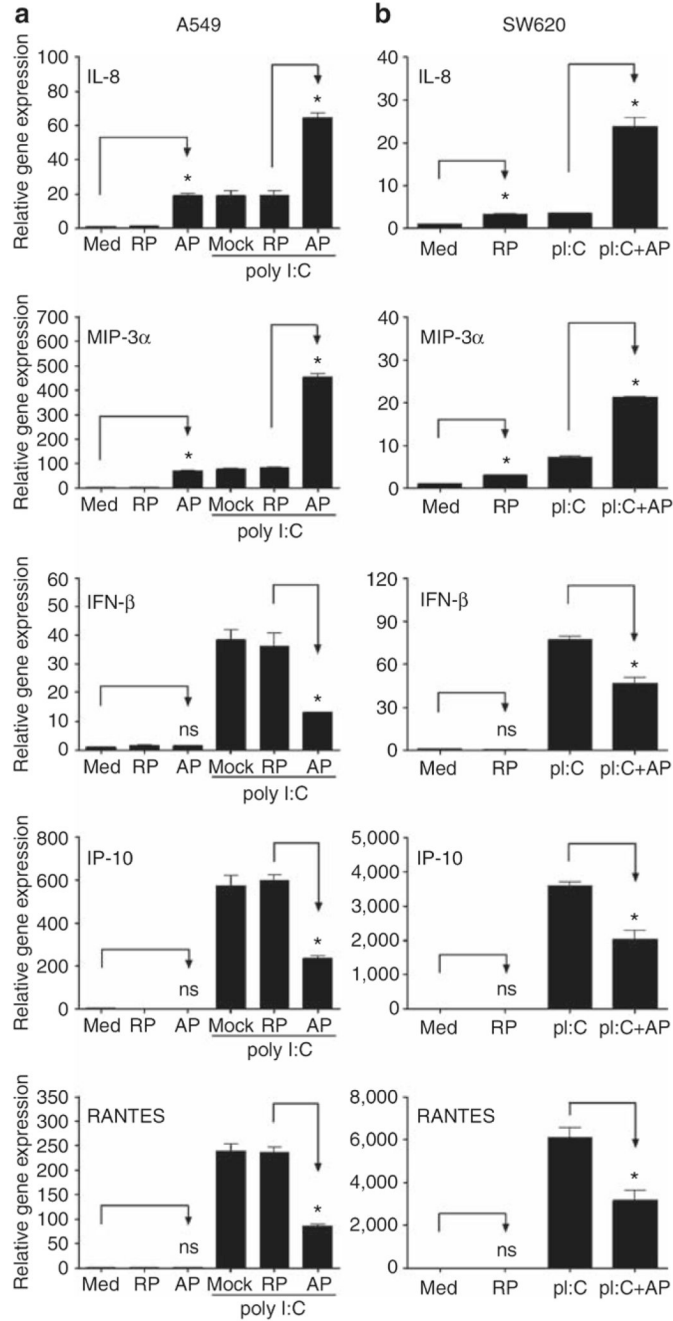


**Figure 3.** Proteinase-activated receptor 2 (PAR<sub>2</sub>) agonist peptide (AP) differentially regulates Toll-like receptor 3 (TLR3) responses in human mucosal epithelial cell lines. Relative gene expression was analyzed by quantitative real-time PCR (qPCR). (a) A549 cells (left panels) were treated with medium (Med), PAR<sub>2</sub> reverse-control peptide (RP), or PAR<sub>2</sub> AP (100 μM), in the absence or presence of poly I:C (100 μg ml<sup>-1</sup>) for 3 h. Data are presented as the mean ± s.d., representative of four separate experiments. (b) SW620 cells (right panels) were treated with medium (Med) or PAR<sub>2</sub> AP (300 μM), in the absence or presence of poly I:C (100 μg ml<sup>-1</sup>) for 3 h. Data are presented as the mean ± s.d., representative of three separate experiments. ns, not significant; \* *p*<0.05.

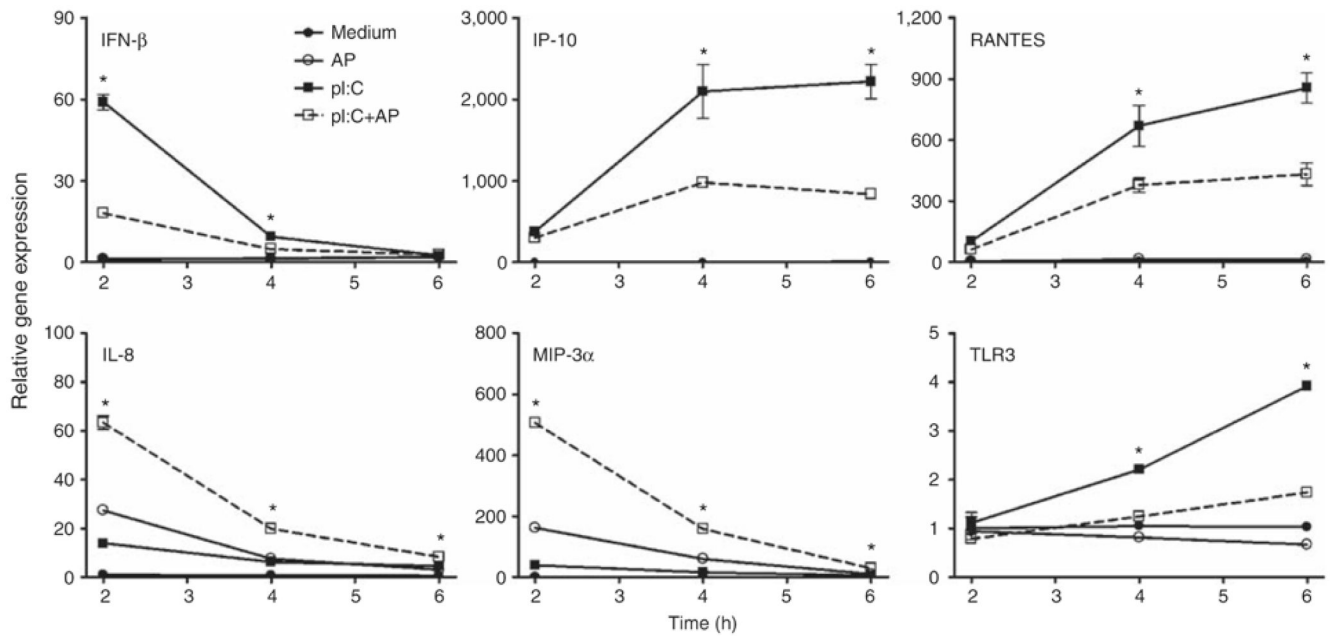


**Figure 4.** Kinetics of proteinase-activated receptor 2 (PAR<sub>2</sub>) agonist peptide (AP)-mediated differential modulation of Toll-like receptor 3 (TLR3) responses in human lung epithelial cell line. A549 cells were treated with medium (closed circles), PAR<sub>2</sub> AP (100 μM; open circles), poly I:C (pI:C; 100 μg ml<sup>-1</sup>; closed squares), or both (open squares/dotted lines) over the indicated time. mRNA was subjected to quantitative real-time PCR (qPCR) analysis. Relative gene expression is presented as the mean ± s.d., representative of three separate experiments. \* *p*<0.05.



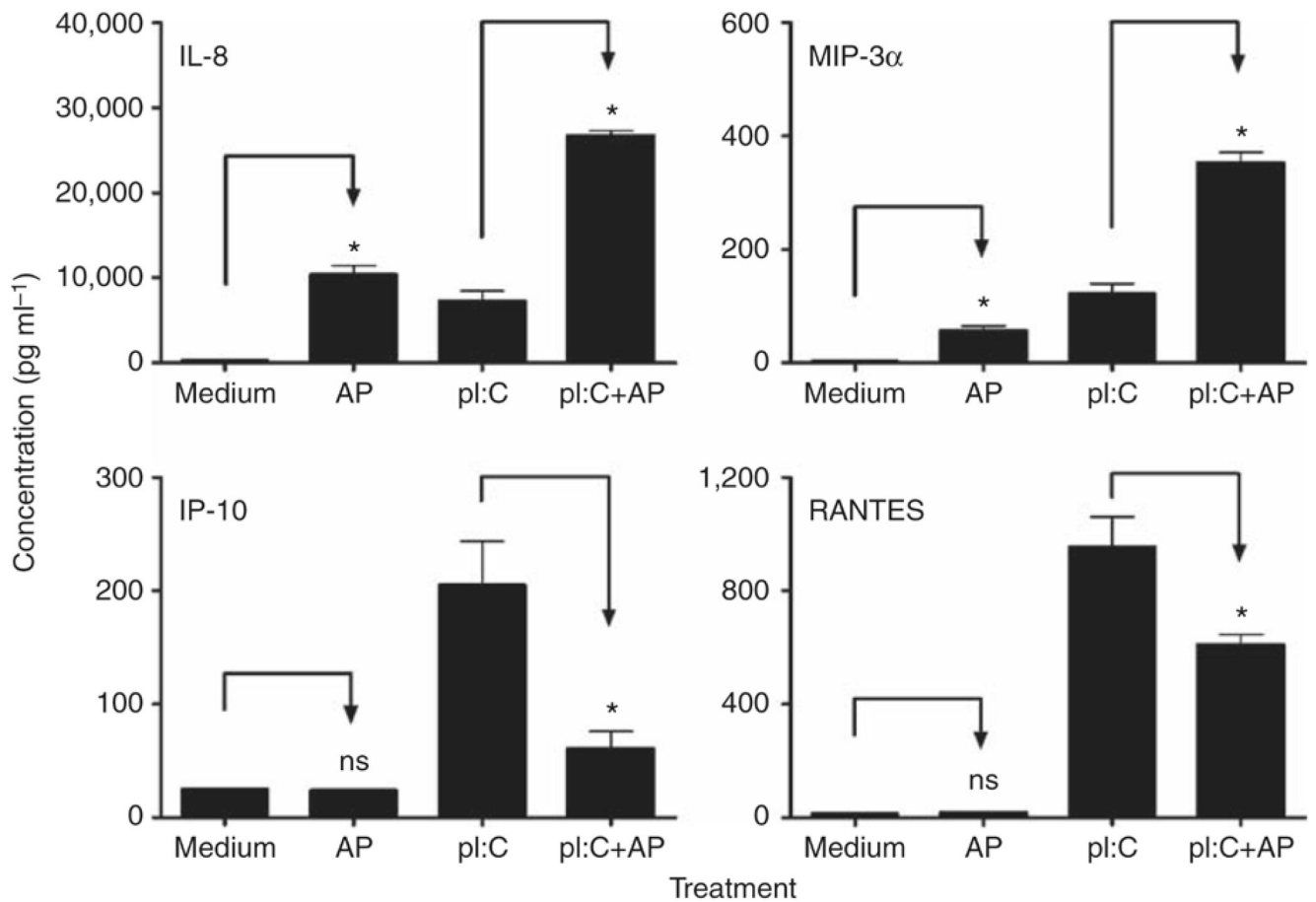


**Figure 5.** Proteinase-activated receptor 2 (PAR<sub>2</sub>) agonist peptide (AP) differentially regulates Toll-like receptor 3 (TLR3)-induced chemokine secretion in human lung epithelial cell line. In all,  $8 \times 10^5$  A549 cells were seeded per well in 24-well plates overnight. Cells were treated with medium, PAR<sub>2</sub> AP (200  $\mu$ M), poly I:C (pl:C; 100  $\mu$ g ml<sup>-1</sup>), or both for 24 h in 0.5 ml volume. Supernatants were collected and analyzed for secreted chemokines by enzyme-linked immunosorbent assay (ELISA). Data are presented as the mean  $\pm$  s.d., representative of three separate experiments. ns, not significant; \*  $p < 0.05$ .

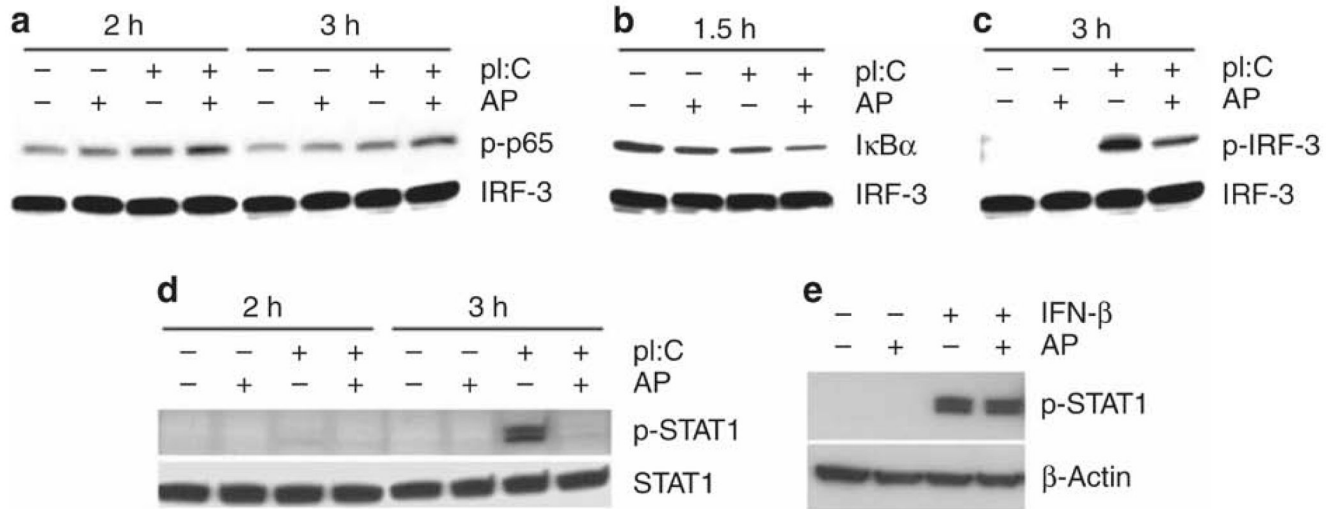


**Figure 6.** Effects of proteinase-activated receptor 2 (PAR<sub>2</sub>) agonist peptide (AP) on Toll-like receptor 3 (TLR3) and interferon (IFN) $\alpha/\beta$ R signaling in human lung epithelial cell (EC) line. **(a–d)** PAR<sub>2</sub> AP differentially regulates TLR3 signaling in human lung EC line. A549 cells were treated with medium, PAR<sub>2</sub> AP (200  $\mu$ M), poly I:C (pI:C; 100  $\mu$ g ml<sup>-1</sup>), or both for the indicated time. Whole-cell lysates were subjected to SDS-polyacrylamide gel electrophoresis (SDS-PAGE) western immunoblot analysis. Data are representative of three separate experiments. **(e)** PAR<sub>2</sub> AP fails to inhibit recombinant IFN- $\beta$  (rIFN- $\beta$ )-induced signal transducer and activator of transcription 1 (STAT1) phosphorylation in human lung EC line. A549 cells were treated with medium, PAR<sub>2</sub> AP (200  $\mu$ M), rIFN- $\beta$  (100 U ml<sup>-1</sup>), or both for 15 min. Whole-cell lysates were subjected to SDS-PAGE western immunoblot analysis. Data are representative of three separate experiments.

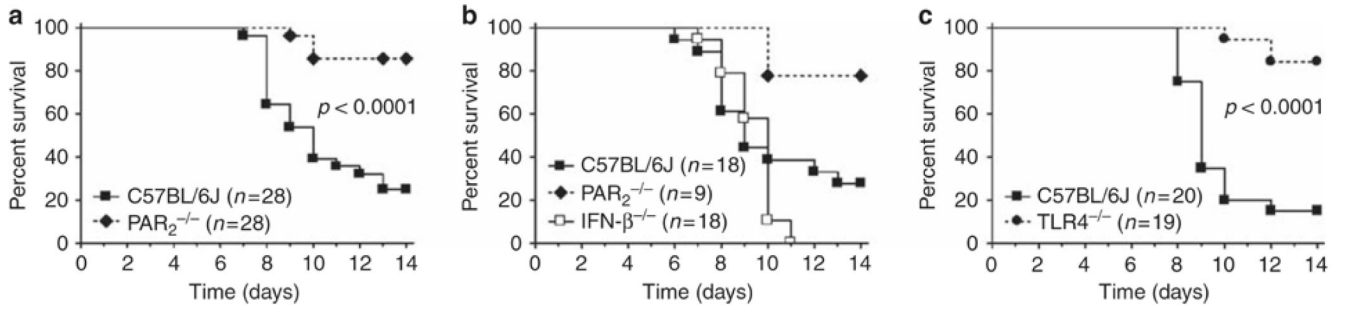


**Figure 7.** Susceptibility of mice to H1N1 influenza A virus-induced lethality. Mice were anesthetized with isoflurane and infected intranasally with 50  $\mu$ l mouse-adapted H1N1 influenza virus (A/PR/8/34; 200 p.f.u. (plaque-forming unit) per mouse) and survival monitored daily for 14 days. **(a)** Survival of  $PAR_2^{-/-}$  and wild-type (WT) C57BL/6J mice infected with influenza A virus. Data are the average of three separate experiments. **(b)** Survival of  $PAR_2^{-/-}$ , interferon (IFN)- $\beta^{-/-}$ , and WT C57BL/6J mice infected with influenza A virus. Data are the average of two separate experiments. **(c)** Survival of  $TLR4^{-/-}$  and WT C57BL/6J mice infected with influenza A virus. Data represent the average of two separate experiments. The total numbers of mice in each infection group are shown in parentheses.

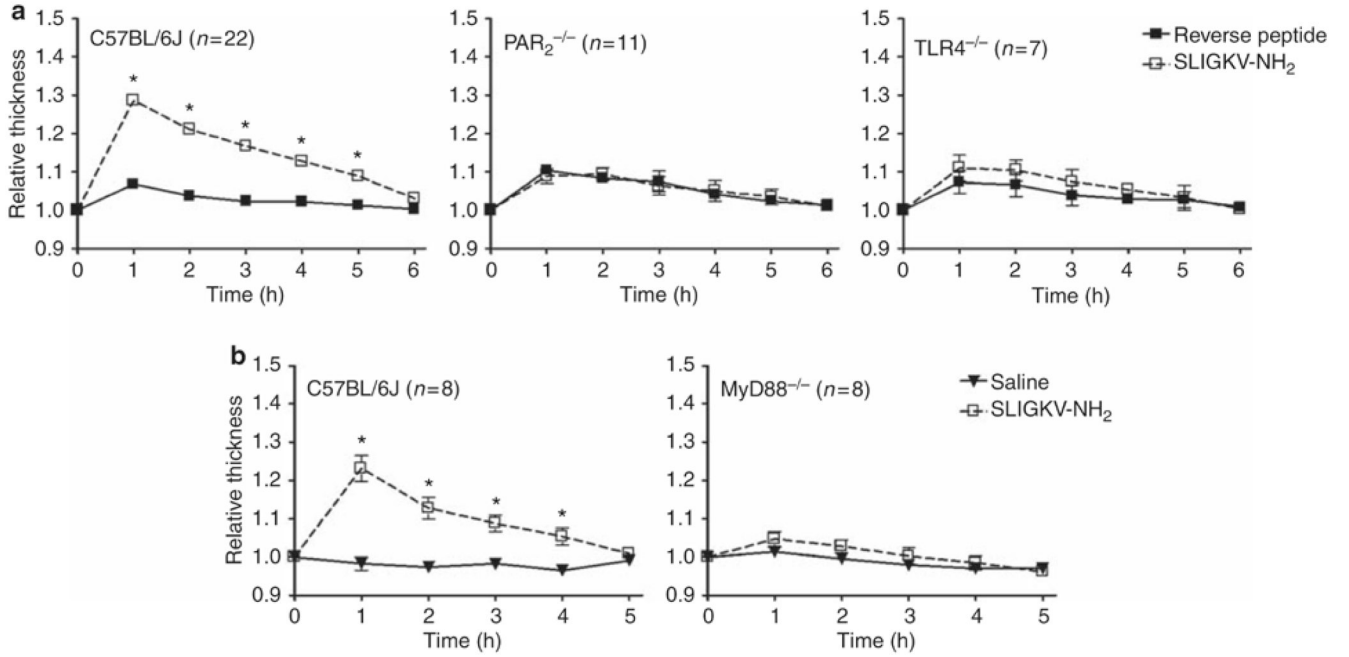


**Figure 8.** Toll-like receptor 4 (TLR4) contributes to proteinase-activated receptor 2 (PAR<sub>2</sub>)-mediated foodpad inflammation *in vivo*. **(a)** Wild-type (WT) C57BL/6J, PAR<sub>2</sub><sup>-/-</sup>, and TLR4<sup>-/-</sup> mice were injected intraplantarly in the hindfoot with PAR<sub>2</sub> agonist peptide (SLIGKV-NH<sub>2</sub>) or reverse-control peptide at 150 μg per 30 μl. Footpad thickness was measured hourly for 6 h using an engineering caliper. Data are the mean ± s.e.m. of two to six separate experiments. **(b)** WT C57BL/6J and MyD88<sup>-/-</sup> mice were injected intraplantarly in the hindfoot with PAR<sub>2</sub> agonist peptide (SLIGKV-NH<sub>2</sub>; 150 μg per 30 μl) or saline. Footpad thickness was measured hourly for 5 h using an engineering caliper. Data represent the mean ± s.e.m. of two separate experiments. \* *P* < 0.05. The total numbers of mice in each treatment group are shown in parentheses.

**Table 1**

Primer sequences of human genes examined by quantitative real-time PCR. AS, antisense; COX-2, cyclooxygenase-2; HPRT, hypoxanthine guanine phosphoribosyltransferase; IFN- $\beta$ , interferon- $\beta$ ; IL-1 $\beta$ , interleukin-1 $\beta$ ; IL-6, interleukin-6; IL-8, interleukin-8; IP-10, 10 kDa interferon- $\gamma$ -induced protein; MCP-1, monocyte chemotactic protein-1; MIP-2 $\alpha$ , macrophage inflammatory protein-2 $\alpha$ ; MIP-3 $\alpha$ , macrophage inflammatory protein-3 $\alpha$ ; RANTES, regulated upon activation, normal T-cell expressed, and secreted; S, sense; TNF- $\alpha$ , tumor necrosis factor- $\alpha$ .

Target gene	Primer sequence
HPRT	5'-CAAGCTTGCTGGTGAAAAGGAC-3' (S) 5'-GTCAAGGGCATATCCTACAACAAA-3' (AS)
IL-8	5'-ATAAAGACATACTCCAAACCTTTCCAC-3' (S) 5'-AAGCTTTACAATAATTTCTGTGTTGGC-3' (AS)
MIP-3 $\alpha$	5'-GCGGCGAATCAGAAGCA-3' (S) 5'-GGCCAGCTGCCGTGTG-3' (AS)
IFN- $\beta$	5'-GGCAATTGAATGGGAGGCT-3' (S) 5'-GGCGTCCTCCTTCTGGAAC-3' (AS)
IP-10	5'-TGACTCTAAGTGGCATTCAAGGAG-3' (S) 5'-TTTTTCTAAAGACCTTGATTAACAGG-3' (AS)
RANTES	5'-TTTGCCTACATTGCCCGC-3' (S) 5'-TTTCGGGTGACAAAGACGACT-3' (AS)
TNF- $\alpha$	5'-CCCAGGGACCTCTCTAATCA-3' (S) 5'-GCTTGAGGGTTTGCTACAACATG-3' (AS)
IL-6	5'-GTAGCCGCCCCACACAGA-3' (S) 5'-CATGTCTCCTTTCTCAGGGCTG-3' (AS)
IL-1 $\beta$	5'-AAATACCTGTGGCCTTGGGC-3' (S) 5'-TTTGGGATCTACACTCTCCAGCT-3' (AS)
MIP-2 $\alpha$	5'-CGCCCAAACCGAAGTCAT-3' (S) 5'-GATTTGCCATTTTTCAGCATCTT-3' (AS)
MCP-1	5'-ACTCTCGCCTCCAGCATGAA-3' (S) 5'-TTGATTGCATCTGGCTGAGC-3' (AS)
COX-2	5'-CCCATGTCAAAACCGAGGTG-3' (S) 5'-CCGGTGTGAGCAGTTTTCTC-3' (AS)